





## Open Archive Toulouse Archive Ouverte (OATAO)

OATAO is an open access repository that collects the work of Toulouse researchers and makes it freely available over the web where possible

This is a Publisher's version published in: <http://oatao.univ-toulouse.fr/24429>

**Official URL:** <https://doi.org/10.1016/j.egypro.2009.01.051>

### To cite this version:

Lambert, Arnold and Delquié, Céline  and Clémeneçon, Isabelle and Comte, Elodie and Lefebvre, Véronique and Rousseau, Jacques and Durand, Bernard   
*Synthesis and characterization of bimetallic Fe/Mn oxides for chemical looping combustion.* (2009) Energy Procedia, 1 (1). 375-381. ISSN 1876-6102

Any correspondence concerning this service should be sent to the repository administrator: [tech-oatao@listes-diff.inp-toulouse.fr](mailto:tech-oatao@listes-diff.inp-toulouse.fr)



GHGT-9

## Synthesis and characterization of bimetallic Fe/Mn oxides for chemical looping combustion

Arnold Lambert<sup>a,\*</sup>, Céline Delquie<sup>b</sup>, I. Cléménçon<sup>a</sup>, Elodie Comte<sup>a</sup>, Véronique Lefebvre<sup>a</sup>, J. Rousseau<sup>a</sup>, B. Durand<sup>b</sup>

<sup>a</sup>IFP-Lyon, Rond-point de l'échangeur de Solaize, BP3, 69360, Solaize, France

<sup>b</sup>CIRIMAT, Université Paul Sabatier, Toulouse, 31062, France

---

### Abstract

Fe-Mn mixed oxides have been prepared by different routes, characterized, and tested with TGA for application as oxygen carriers in the CLC process. These mixed oxides exhibit a lower oxygen transfer capacity than Ni based materials which is also dependant on synthesis method.

In-situ XRD analysis was performed with one sample and allowed to clearly demonstrate the reaction pathway, reduction and oxidation reactions occurring stepwise, with little phase coexistence. SEM-EDS analysis on reduced and re-oxidized samples show atom migration occurs on a rather long distance, forming Fe<sup>0</sup> and MnO particles during reduction which are oxidized back to (Fe,Mn)<sub>2</sub>O<sub>3</sub>.

© 2009 Elsevier Ltd. Open access under [CC BY-NC-ND license](https://creativecommons.org/licenses/by-nc-nd/4.0/).

**Keywords:** Chemical looping combustion; CLC; CO<sub>2</sub> capture; Iron; Manganese; Mixed oxides

---

### 1. Introduction

Electricity production through chemical looping combustion (CLC) of fossil fuels is a promising technology which generates hot oxygen depleted air and CO<sub>2</sub>/H<sub>2</sub>O streams, hence allowing CO<sub>2</sub> capture at low energy penalty [1]. The technology relies on the circulation of metallic oxides which transfer oxygen from an air reactor to a fuel reactor. The oxide particles are reduced in the fuel reactor by e.g. natural gas or coal, producing CO<sub>2</sub> and steam. and they are oxidized back in the air reactor. In order to circulate these oxides between both reactors using the fluidized bed technology, they have to be highly chemically and mechanically resistant, and their reactivity under oxidizing and reducing conditions should be high to lower the inventory of material.

\* Corresponding author Tel : +33 478 022 930; fax: +33 478 022 060

E-mail address: [arnold.lambert@ifp.fr](mailto:arnold.lambert@ifp.fr)

From the many oxygen carriers that have been studied, nickel oxide seems to be the most appropriate for use in CLC application. However, like most oxides, the use of a ceramic, unreactive, binder is necessary to increase its mechanical resistance. Furthermore, toxicity and cost considerations have led many research teams around the world to look for alternative oxygen carriers showing performances similar to or better than nickel oxide.

Iron and manganese oxide particles have been widely studied as single metallic oxides, in association with different binders [2, 3]. Both metals exhibit different oxydo-reduction couples, each one of them behaving differently under CLC conditions. Hence,  $\text{Fe}_2\text{O}_3/\text{Fe}_3\text{O}_4$  is very reactive,  $\text{Fe}_3\text{O}_4/\text{FeO}$  has moderate activity, and  $\text{FeO}/\text{Fe}$  is hardly reactive. For manganese,  $\text{MnO}_2$  decomposes at  $460^\circ\text{C}$  and cannot be used at CLC temperatures, and  $\text{Mn}_2\text{O}_3$  decomposes at  $802^\circ\text{C}$ , rendering its study rather difficult. The  $\text{Mn}_3\text{O}_4/\text{MnO}$  couple is rather active, and the reduction  $\text{MnO} \rightarrow \text{Mn}$  at CLC temperature levels is not observed, in agreement with thermodynamics.

In this work, we studied iron-manganese mixed oxides to check for eventual cooperative effects between both metals. Several Fe-Mn mixed oxides have been prepared according to different synthesis schemes and characterized. The oxygen transfer capacity of the materials was measured on a thermobalance at  $900^\circ\text{C}$  using methane as fuel and air as oxidant, and compared with that of NiO-YSZ (Yttria Stabilized Zirconia). In situ XRD was used to follow the phase transformations during reduction and oxidation periods.

## 2. Experimental

### 2.1. Mixed oxides synthesis

NiO-YSZ (57%-43%) was prepared by co-precipitation of nickel, yttrium and zirconyl nitrate with sodium hydroxide. The precipitate was filtered, washed with water, dried at  $120^\circ\text{C}$ , and calcined at  $1000^\circ\text{C}$  for two hours.

Mn-Fe mixed oxides were prepared by oxalate co-precipitation of chlorinated or sulphate precursors in water or in a water-ethylene glycol mixture (60-40). A solution was prepared by dissolving the iron and manganese chloride or sulphate precursors in water or hydro alcoholic medium solvent (60vol % water/40vol % ethylene glycol). This solution was mixed with an aqueous or alcoholic solution of oxalic acid and stirred for 30 minutes. The precipitate was then filtered and washed with water, dried overnight at  $90^\circ\text{C}$  and summarily crushed to obtain the oxalate powder. This powder was then heated in air at  $1000^\circ\text{C}$  for two hours ( $150^\circ\text{C}\cdot\text{h}^{-1}$  heating rate) to decompose the oxalates into oxides. Details of the synthesized oxides are given in Table 1.

Mn-Fe mixed oxides were also prepared by hydrothermal synthesis using nitrate precursors. A solution was prepared by dissolving the iron and manganese precursors in water. The pH of this solution was raised above 12 by KOH (1,5M) addition under continuous stirring. The hydroxide mixture obtained was poured into a 120 mL Teflon-lined stainless-steel autoclave. The autoclave was placed inside an oven maintained at  $150^\circ\text{C}$  for 18 hours. The autoclave was then cooled at room temperature, and the powder product was filtered and washed with distilled water. It was oven dried at  $90^\circ\text{C}$  overnight and then crushed with a mortar. The powder was then calcined at  $1000^\circ\text{C}$  for two hours.

### 2.2. Characterization

ICP analyses were performed on an ICP-AES - JOBIN YVON spectrometer.

BET surface area measurements were performed on a Micromeritics ASAP2410 apparatus, using  $\text{N}_2$  as a probe.

XRD analysis of the prepared oxides was performed using a Brucker D4 Endeavor Diffractometer in Bragg-Brentano configuration ( $\text{CuK}\alpha$  radiation).

SEM-EDS analysis of oxidized and reduced AQ60-40 was performed on a CARL ZEISS SUPRA 40 microscope

Table 1 : syntheses parameters for oxalate co-precipitation

Method	Media	Precursors	Samples (Xmol% Mn-Ymol% Fe)
Oxalate coprecipitation	hydro alcoholic	chlorides	ALC0-100; ALC20-80; ALC60-40
	aqueous	chlorides	AQ0-100; AQ10-90; AQ20-80; AQ40-60; AQ90-10; AQ100-0
		sulphates	AQSULF25-75; AQSULF50-50; AQSULF75-25
hydrothermal synthesis	aqueous	nitrates	SH25-75; SH50-50; SH75-25

In-situ XRD analysis was performed on the AQ60-40 sample, using hydrogen as reducing gas, at 700°C, and air as oxidising gas, with PANalytical's X'Pert PRO diffractometer equipped with Anton Paar's XRK900 reactor chamber. The sample was initially heated under air up to 700°C, a nitrogen purge was then performed before switching to hydrogen gas. Diffraction patterns were recorded every three minutes for one hour, then the cell was purged with nitrogen and the gas was switched back to air. Diffraction patterns were again recorded every three minutes for one hour.

### 2.3. Chemical looping combustion behavior simulation

A Setaram thermobalance was used to measure the oxygen transfer capacity (OTC) of the samples. The tests were performed at 900°C, using  $65 \pm 2$  mg sample (sieved between 30 and 40  $\mu\text{m}$ ) placed in a platinum crucible. Gas flows of 80 ml/min were used. The reduction gas was composed of 10%  $\text{CH}_4$ , 25%  $\text{CO}_2$  and 65%  $\text{N}_2$ , and dry air was used as oxidation gas. Nitrogen flushing was systematically performed for 5 minutes between the oxidizing and reducing periods. For each sample, five consecutive reduction(20 min)/oxidation(20min) cycles were performed.

## 3. Results and discussion

ICP analysis of the various samples shows that iron and manganese are present in the initial ratio for the hydrothermal syntheses. A slight deviation to initial stoichiometry is observed for the oxalate coprecipitated samples, with more Mn detected than iron.

Regardless of preparation mode, the measured BET surface area of the Mn-Fe mixed oxides was systematically lower than 5  $\text{m}^2/\text{g}$ , due to the high calcination temperature. Also independent of preparation mode, XRD analysis shows that samples containing 10 to 25mol % Mn exhibit two phases: a bixbyite type phase ( $\text{Mn}_2\text{O}_3$ ) with iron inclusion, and a hematite type phase ( $\text{Fe}_2\text{O}_3$ ) with Mn inclusion. For samples with 40mol% Mn or more, only the iron containing bixbyite phase is observed.

Oxygen transfer capacities (OTC) measured by TGA are shown in figure 1. No clear trend as to which method and compositions give the best oxygen transfer capacity can be obtained from TGA tests. All the prepared samples show a lower OTC than the reference NiO/YSZ sample.

Unfortunately, reduction and oxidation rates, which can also be extracted from TGA traces, are not significant as it was realized that diffusional limitations occur under our test conditions. However, the shape of the weight variations observed under cyclic conditions depends both on preparation mode and on materials' composition. In materials containing between 50 and 100% Mn (figure 2), while reduction by methane is rather fast and monotonous, oxidation by air occurs in two successive steps: at first, fast oxidation is observed, followed by a second oxidation stage which is much slower and incomplete in the time imparted to the oxidation period.

Interestingly, when no iron is present, this second oxidation step is not observed at all. Materials with less than 50% Mn are oxidized back to their initial weight in a single step.

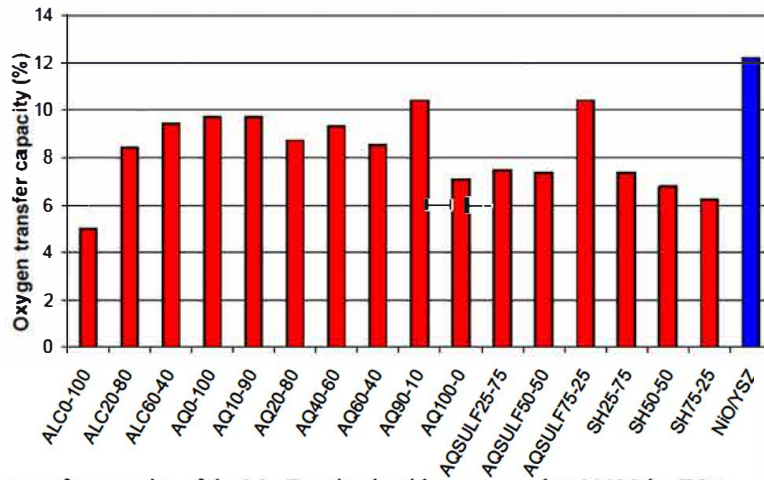


Figure 1: oxygen transfer capacity of the Mn-Fe mixed oxides measured at 900°C by TGA

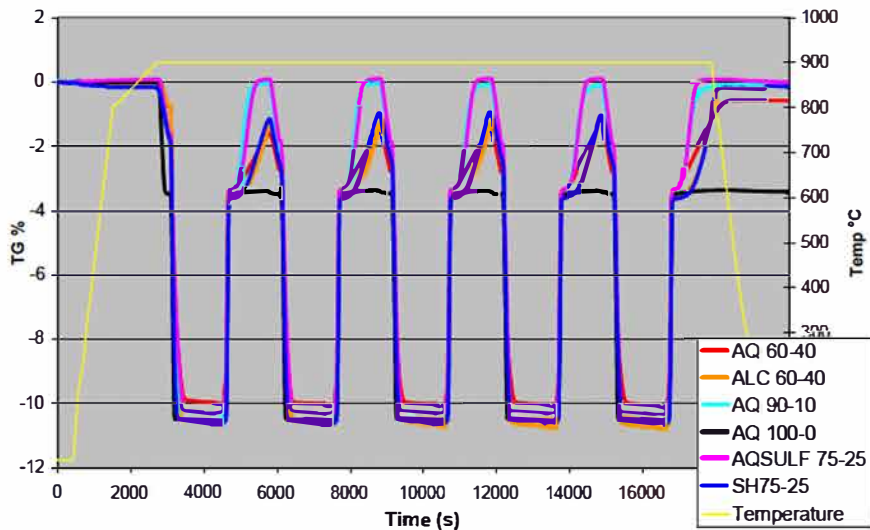


Figure 2 : TGA traces of samples containing between 50 and 100 mol % Mn

X-ray diffraction diagrams obtained during the in-situ reduction of AQ60-40 are shown in figure 3. During the first six minutes under hydrogen, only the initial iron containing bixbyite phase is observed. Part of the delay observed here can be attributed to the time necessary to renew the atmosphere in the reactor chamber. After 9 minutes, peaks corresponding to  $(\text{Mn},\text{Fe})\text{O}$  and  $(\text{Mn},\text{Fe})_3\text{O}_4$  phases are observed. 12 minutes into reduction,  $(\text{Mn},\text{Fe})_3\text{O}_4$  diffraction peaks have already disappeared, and only peaks from the  $(\text{Mn},\text{Fe})\text{O}$  phase are present. From 15 minutes onwards to 60 minutes reduction time, the  $(\text{Mn},\text{Fe})\text{O}$  phase is still present, and a metallic phase gradually appears. In that period of time, the position of the  $(\text{Mn},\text{Fe})\text{O}$  peaks moves progressively towards smaller angles, indicating that the cell parameter of the phase is growing. Since the ionic radius of  $\text{Fe}^{2+}$  (0.61 Å) is smaller than that of  $\text{Mn}^{2+}$  (0.83 Å), it is likely that the  $(\text{Mn},\text{Fe})\text{O}$  structure is belching out iron atoms, which form metallic iron particles big enough to be detected by XRD. This implies rather long distance migration of iron atoms. Such

migration was confirmed by SEM-EDX characterization of the as-prepared and the reduced sample. In the as-prepared (oxidized) sample, iron and manganese are homogeneously distributed, as shown in figure 4. In contrast, the SEM-EDS cartography (figure 5) of the sample reduced at 700°C with H<sub>2</sub> in the TGA clearly shows that iron and manganese are forming distinct clusters. ~200 nm wide iron particles are clearly formed at the reduction temperature of 700°C. The metallic iron particles are nested within a manganese oxide framework, which still contains iron. This is probably due to the fact that the reduction of the sample analysed by SEM was not complete, and the pure MnO phase observed by in-situ XRD after an hours' reduction could not form in the twenty minutes reduction time used in the ATG reduction. Indeed, the MnO cell parameter only stabilizes after about 35 minutes reduction. Furthermore, the sample analyzed by SEM had lost only 17.6wt % when TGA reduction was stopped, whereas full reduction to MnO + Fe<sup>0</sup> would correspond to an 18.2% weight loss.

The fact that the (Mn,Fe)<sub>3</sub>O<sub>4</sub> phase is only observed during the third XRD acquisition under H<sub>2</sub> implies that it is quickly reduced to the (Mn,Fe)O phase, while the later reduces much slower to MnO + Fe<sup>0</sup>.

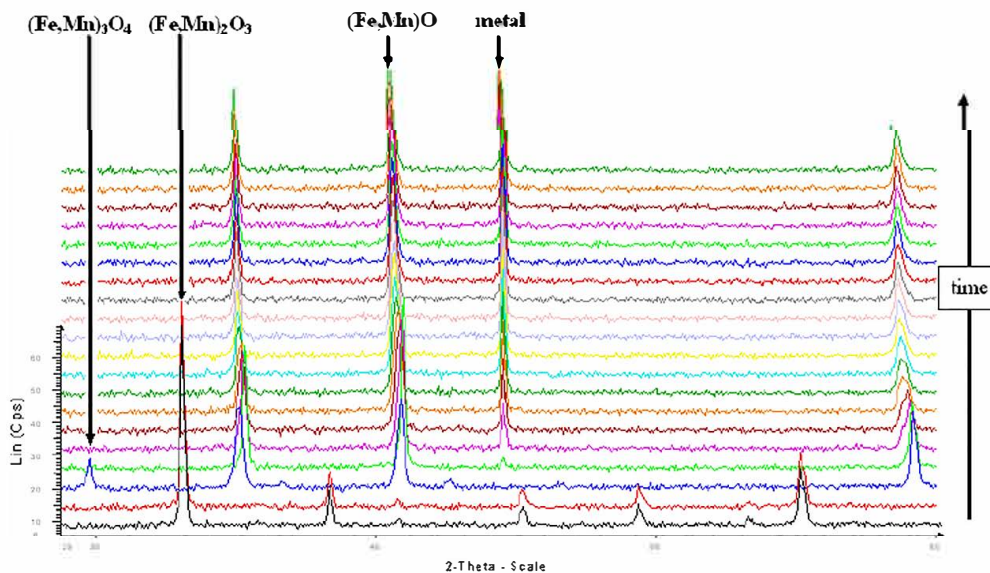


Figure 3 : diffractograms recorded in-situ during the reduction of AQ60-40 by H<sub>2</sub> at 700°C.

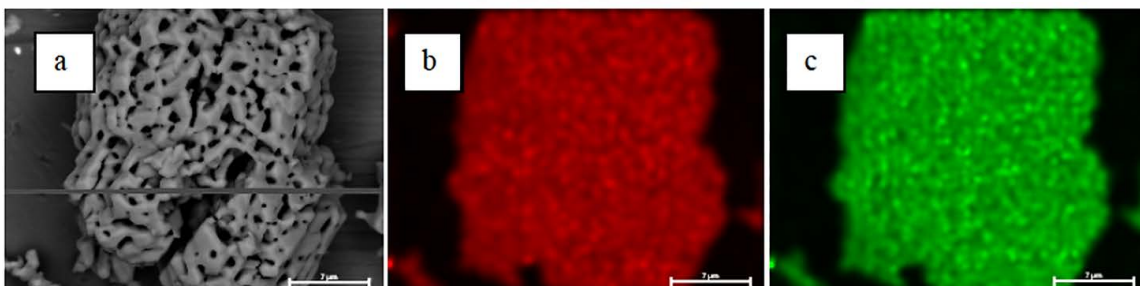


Figure 4: SEM-EDX analysis of as-prepared AQ60-40. a: chemical contrast; b: Fe distribution; c: Mn distribution

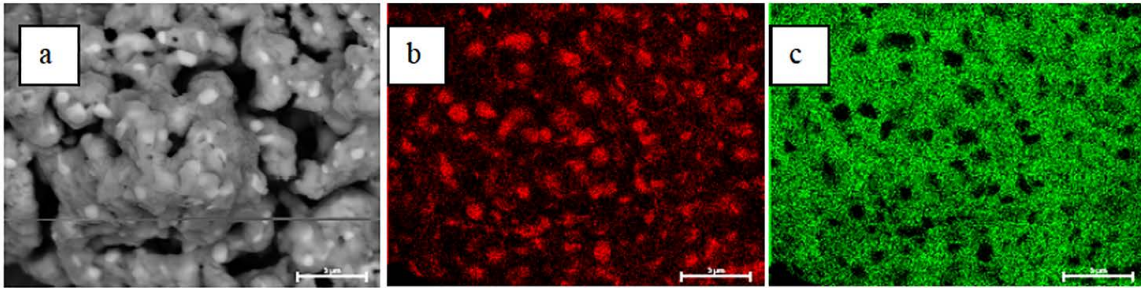


Figure 5: SEM-EDX analysis of reduced AQ60-40. a: chemical contrast; b: Fe distribution; c: Mn distribution

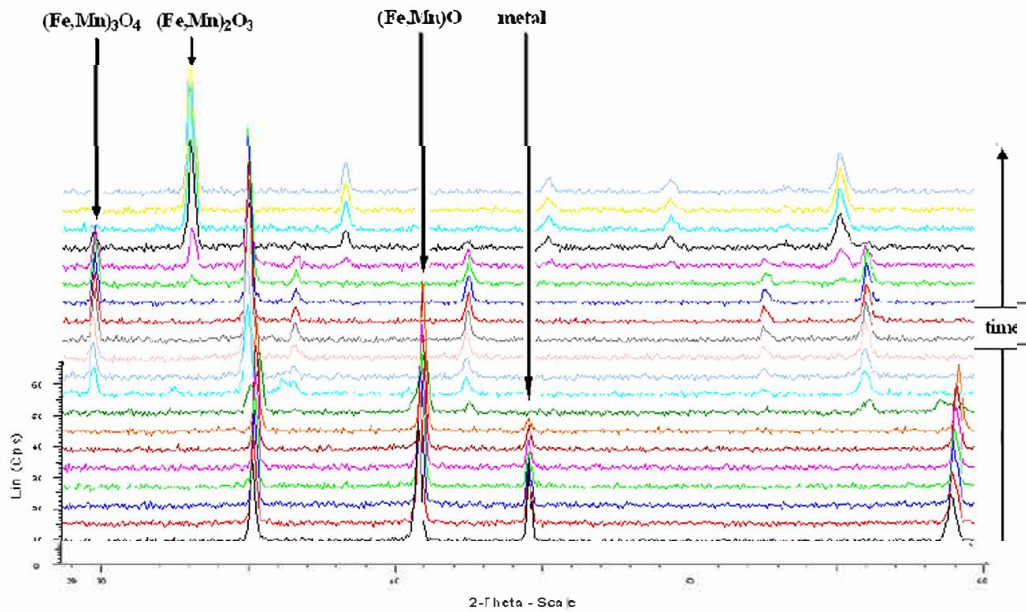


Figure 6 : diffractograms recorded in-situ during the oxidation of reduced AQ60-40 by air at 700°C

Upon re-oxidation of the sample (figure 6), the metallic iron peak disappears slowly at 700°C under air, with concomitant apparition of a (Mn,Fe)O solid solution which incorporates more and more iron with time. When the metallic phase disappears (after about 20 minutes oxidation), the (Mn,Fe)O phase is fairly quickly oxidized back to (Mn,Fe)<sub>3</sub>O<sub>4</sub> (the (Mn,Fe)O peaks disappear within 10 minutes). The (Mn,Fe)<sub>3</sub>O<sub>4</sub> phase is stable for about 20 minutes, after which it oxidizes back to the initial (Mn,Fe)<sub>2</sub>O<sub>3</sub> structure. The reason for such a delay in oxidation of the (Mn,Fe)<sub>3</sub>O<sub>4</sub> is not clear. It could be due to the need for the Mn and Fe ions to reach a certain distribution within the spinel structure of (Mn,Fe)<sub>3</sub>O<sub>4</sub>, which requires time at high temperature to occur.

Complete reduction of the AQ60-40 sample according to reactions 1 to 3 below corresponds to a theoretical oxygen transfer capacity of 18.2% :

Reaction 1	(Mn,Fe) <sub>2</sub> O <sub>3</sub>	(Mn,Fe) <sub>3</sub> O <sub>4</sub>	(3.33 %)
Reaction 2	(Mn,Fe) <sub>3</sub> O <sub>4</sub>	(Mn,Fe)O	(6.78 %)
Reaction 3	(Mn,Fe)O	MnO + Fe <sup>0</sup>	(8.05 %)

AQ60-40 shows a first weight loss of 10% upon TGA reduction by methane at 900°C, which could be due to partial reduction of the sample from  $(\text{Mn,Fe})_2\text{O}_3$  to  $(\text{Mn,Fe})\text{O}$  (3.33% + 6.78% = 10.1% weight loss). This is supported by the fact that the first re-oxidation step in TGA is rather fast, in this way corresponding to what was observed by in-situ XRD oxidation (fast oxidation of  $(\text{Mn,Fe})\text{O}$  to  $(\text{Mn,Fe})_3\text{O}_4$ ). Also, the first re-oxidation step observed by ATG corresponds to a 6.6wt % increase, matching roughly the weight increase between  $(\text{Mn,Fe})\text{O}$  and  $(\text{Mn,Fe})_3\text{O}_4$ .

The second, slow oxidation step is incomplete in the first four TGA cycles, probably due to the fact they are too short, but at the end of the fifth cycle, the sample is left under air for a longer period of time and regains its initial weight, hence completing oxidation of  $(\text{Mn,Fe})_3\text{O}_4$  to  $(\text{Mn,Fe})_2\text{O}_3$ .

Further supporting the assumption that methane does not reduce the  $(\text{Mn,Fe})\text{O}$  phase to  $\text{Fe}^0 + \text{MnO}$  at 900 °C is the fact that when submitted to TGA conditions at 700°C under  $\text{H}_2$  and under methane, AQ60-40 shows a 17.6 % weight loss and 4.6 % weight loss, respectively. Hydrogen is hence confirmed as a much better reducer than methane.

#### 4. Conclusions

Several Mn-Fe mixed oxides were synthesized and characterized. Materials with the same Mn/Fe ratio prepared by the different methods show no structural differences as analyzed by XRD. Such materials however behave differently when cycled between methane and air in a TGA test at 900°C. Their oxygen transfer capacity is always lower than that of nickel oxide based particles.

$(\text{Mn,Fe})_2\text{O}_3$  samples containing between 50 and 100 mol % manganese are reduced by methane at 900°C via an intermediate  $(\text{Mn,Fe})_3\text{O}_4$  spinel phase which reduces very fast to  $(\text{Mn,Fe})\text{O}$ . Further reduction to manganese oxide (MnO) and metallic iron can be observed when hydrogen is used as a reducer.

Upon re-oxidation, the inverse pathway occurs. Starting from a deeply reduced sample ( $\text{MnO} + \text{Fe}^0$ ), the metallic phase is inserted in the MnO phase to form a solid solution. The latter then fairly quickly oxidises back to  $(\text{Mn,Fe})_3\text{O}_4$ . An induction time is then observed before the spinel phase oxidises back to  $(\text{Mn,Fe})_2\text{O}_3$ . The origin of the induction period is not fully understood.

[1] M. Ishida, H. Jin, J. Chem. Eng. Jap 27 (1994), 296; M. Ishida, H. Jin, T. Okamoto, Energy and Fuels 10 (1996) 958.

[2] J.S. Dennis, S.A. Scott, A.N. Hayhurst, J. Energy Institute, 79 (2006) 187; S.R. Son, S.D. Kim, Ind. Eng. Chem. Res. 45 (2006) 2689.

[3] M. Johansson, T. Mattison, A. Lyngfelt, Thermal Science 10 (2006) 93; M. Johansson, T. Mattison, A. Lyngfelt, Chem. Eng. Res. Design 84 (2006) 807